Kinetics of Carbide Formation During Ageing of Pearlitic 12X1МФ Steel

Arūnas BALTUŠNIKAS∗, Rimantas LEVINSKAS, Irena LUKOŠIŪTĖ

Lithuanian Energy Institute, Breslaujos 3, LT-44403 Kaunas, Lithuania

Parameters of carbide phase electrochemical separation in electrolytes solutions of pearlitic 12X1МФ heat resistant steel, used in thermal power plants facilities are presented in the article. The most relevant electrolyte is chosen and its concentration is specified. Operated and under laboratory conditions aged steel surface microstructure and morphology were evaluated by optic and scanning electron microscopy methods. Using electrochemical etching and XRD qualitative analysis of carbide compounds of 550 °C exploited steel and aged under laboratory conditions at 600, 650, 700 °C from 24 h up to 864 h was carried out. Kinetics of carbides formation is given in mathematical equations. It was determined that during exploitation and ageing samples at 700 °C for 576 h the steel pearlite completely decomposes, whereas alloy elements diffuse into intergrain area thus forming special alloy carbides. Experiments revealed that the XRD analysis of electrochemically separated carbide phase is a rapid and informative method of evaluation the service condition of steel.
Keywords: heat resistant steel, carbide, heat treatment, kinetic, electrochemical etching, XRD.

INTRODUCTION

Low alloy steels of Cr-Mo-V types are extensively used for various engineering components in thermal power plants of China, India, Poland, Russia and former Soviet Union countries like Ukraine, Lithuania and others. The pipelines of power plants mostly are made of 12X1МФ (Russian grade) or 12Kh1MF (in English) steel (GOST 5520, 1979) equivalent to 13HMF (Polish standard), or 14CrMo4-5 (ISO 9328-2, 1991), or 13CrMo4-5 (EN 10028-2, 1992), or F12C1.1 (ASTM A182-96). The chemical composition of 12X1МФ steel is: 0.12 % C, 1.1 % Cr, 0.54 % Mn, 0.26 % Mo, 0.26 % Si, 0.17 % V, 0.019 % S and 0.015 % P [1]. The initial microstructure of power plant alloy 12X1МФ consists of ferrite-pearlite or ferrite-bainite as the major phases obtained following a hardening and normalizing heat treatment later on sub-jected to very severe tempering (~650 °C…700 °C for several hours) generating the overall coarsening and the precipitation of ever more stable alloy carbides and intermetallic compounds (Fig. 1, curve 1), witch interfere with the progress of dislocations. These solid state reactions eventually determine the properties and mechanical stability of the power plant steels (for example, the resistance to creep deformation) and their useful design lifetimes [1 – 3].

In the heat and power generating plants, the pipelines are used to transport superheated steam in the temperature range 500 °C – 560 °C and under a pressure, $P = 10$ MPa – 15 MPa. During long time service in creep regime to such conditions the microstructure of steel changes, pearlite/bainite decomposes as well as carbides precipitation at the grain boundaries and carbides coarsen-ing processes proceed (Fig. 1, curve 2). Structure changes cause formation of cavities and development of internal damages [4]. It is well known that there is a close coher-ence between changes in microstructure and deterioration of mechanical properties, however, the accurate relation

for creep rupture strength deterioration regarding the microstructural degradation is not yet determined [5, 6].
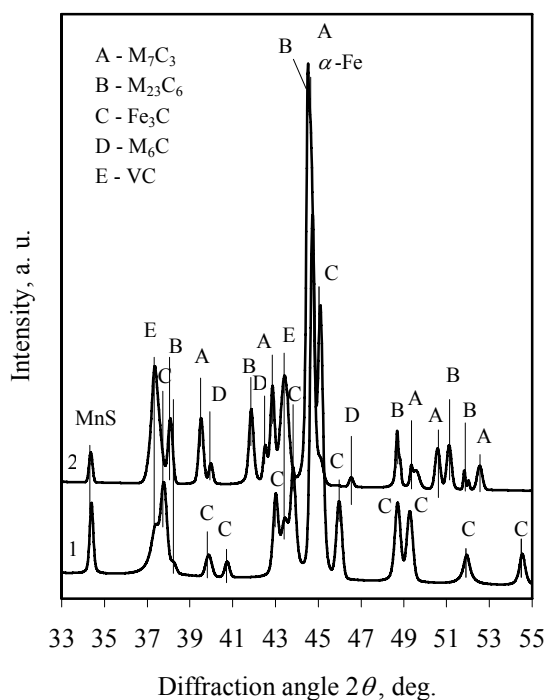

Fig. 1. X-ray diffraction patterns of 12X1МФ virgin (curve 1) steel and exploited 227000 h at 550 °C temperature and pressure of 14 MPa (curve 2)

The original design service life of many power stations in Lithuania and other countries has already been depleted. So, for purpose to ensure safe, reliable and extended op-eration of power plant the prediction of the remaining creep life of power generation plant components which have been in service at elevated temperatures in large part of their design lifetimes is of great significance [7]. For selection suitable failure criteria and testing technique the knowledge of material's characteristics and their variation with time as well as service stresses and temperatures are required. However, the data of service temperature and
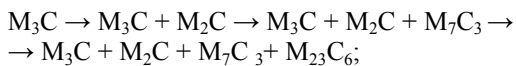
∗Corresponding author. Tel.: +370-37-401905; fax.: +370-37-351271.
E-mail address: *abalt@mail.lei.lt* (A. Baltušnikas)

service time could considerable scatter due to changes of plant operation regime. Therefore, it has been proposed that service time and temperature dependent microstructural parameters, such as quantity and composition of carbides phases, can be used to estimate the thermal history of power plant components at any time during service [5, 8]. To achieve exhaustive information on the alloy steel microstructure stability and to be able to simulate the creep behaviour of the steel knowing only the composition, heat treatment and service conditions, the carbide precipitation sequence that occur in different power plant steels over long periods of time at elevated temperatures was investigated [1, 2, 4 – 6, 8 – 19] and time-temperature-transformation (TTT) diagrams were produced which can be used in remnant life assessments [8]. The precipitation sequence in steel 2.25Cr-1Mo was first determined by Baker and Nutting [20]. Other researchers have shown that there are significant differences in the evolution of carbide precipitation in different steels even when the thermodynamic driving forces are apparently similar. Thus, in [4] it was shown that the difference in the precipitation kinetics of $M_{23}C_6$ in the 3Cr1.5Mo steel and the 2.5Cr1Mo steel is due to the considerably lower driving force for $M_{23}C_6$ in the 2.5Cr1Mo.
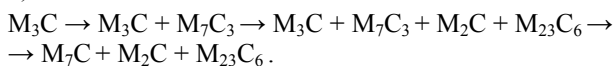
Steels destined for power plant applications might contain any of the following precipitates: iron base carbides or carbonitrides (M_3C, $M_{2.4}C$ and etc.), M(C, N), M_2(C, N), M_7C_3, $M_{23}C_6$, M_5C_2, M_6C, graphite and Laves phase (M stands for metallic solute atom).

It was determined in [21] that the precipitation sequences at 600 °C for steels are as follows:
a) steel 2.25Cr1Mo
$$M_3C \rightarrow M_3C + M_2C \rightarrow M_3C + M_2C + M_7C_3 \rightarrow$$
$$\rightarrow M_3C + M_2C + M_7C_3 + M_{23}C_6;$$
b) steel 3Cr1.5Mo
$$M_3C \rightarrow M_3C + M_7C_3 \rightarrow M_3C + M_7C_3 + M_2C + M_{23}C_6 \rightarrow$$
$$\rightarrow M_7C + M_2C + M_{23}C_6.$$
The same sequence was observed at 650 °C [21].

The purpose of the present work was to investigate the carbides precipitation kinetics of power plant heat resistant steel 12X1МФ during ageing at elevated temperatures and to determine any microstructural parameters that may be used to estimate service history and may be practicable for assessment of remnant life of steel.

METHODOLOGY OF EXPERIMENTS

Investigated 12X1МФ steel was taken from a thick section of superheated steam pipes originally supplied by SC "Lietuvos elektrinė". The samples were prepared from virgin and exploited for 227000 h at 14 MPa pressure and 550 °C – 560 °C steel. Using a potentiostat PI-50-1 and a programmer PER-8 steel anodic polarization curves (e.g. dependence of operating electrode potential on current density) were recorded in solutions of different electrolytes, electrochemical etching solutions and the parameters (critical current density, critical potential) were determined.

The samples (60 mm × 20 mm × 20 mm, working area 2.2 cm^2 ÷ 2.5 cm^2) of 12X1МФ steel were soaked into 20 °C electrolyte solution and current measurements were carried out according argentums chloride reference electrode (EVL – 1M3.1), when the sample potential from the stationary value to 1.2 V varied at $1 \cdot 10^{-3}$ V/s or $5 \cdot 10^{-3}$ V/s rate. Performing anodic polarization of heat resistant steel, Fe ions, which forms insoluble bivalent and then trivalent ferrous hydroxides ($Fe(OH)_2$, $Fe(OH)_3$), enter the electrolyte solution. In order to escape pollution of electrolyte solution oxalic and citric acids, which forms soluble ferrous citrates and oxalates with $Fe(OH)_3$, were used:
$$Fe(OH)_3 + (CH_2COOH)_2C(OH)COOH \rightarrow$$
$$\rightarrow [(CH_2COOH)_2C(OH)COOH]Fe(OH)_3.$$
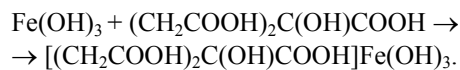
Anodic polarization curves were recorded in 0.05 % and 0.5 % hydrochloric acid solution and in hydrochloric solution with 0.01 % and 0.05 % oxalic or citric acid concentrations.

Power supply 1621A BK Precision was used for electrochemical etching of the steel samples (measurements 20 mm × 10 mm × 10 mm). Electrochemical etching lasted for 1 hour. Samples taken from the etching solution were washed by warm water weak flush and dried in a hot air stream. Under laboratory conditions samples of 12X1МФ steel were aged in electric furnace SNOL 30/1300, in which temperature is automatically regulated from 50 °C to 1300 °C with an accuracy ±4 °C. The samples were isothermally aged at 600, 650 and 700 °C for 24, 48, 192, 288, 384, 576 and 864 h.

The XRD analysis was performed using a diffractometer DRON-UM2 (Russian design). Diffraction patterns were recorded at 30 kV and 20 mA in 1 °/s detector's movement speed, the scanning was carried out with a step length of 0.02° (2θ). Flat diffracted beam pyrolitic graphite monochromator was used to separate CuK$_\alpha$ radiation and to remove undesired radiation (K$_\beta$), high-level bremsstrahlung and radiation due to fluorescence. The diffraction patterns were obtained automatically by a data acquisition system. The peaks recorded were identified with those available in PDF-2 data base [22]. The XRD patterns were refined with a program XFIT, using a pseudo-Voigt function for line profiles modelling [23].

Results of XRD analysis of heat resistant 12X1МФ steel were compared with the metallographic experiments of microstructure and morphology of samples' surface, which were carried out by an optic microscope "Olympus" with video camera Sony DXC-151 AP and NIH Image 1.61 software and scanning electronic microscope JSM 5600, the resolution of which 3.5 nm, accelerating voltage 30 kV.

Mechanical grinding of the samples was done in Buechler Ecomet II device. Polishing was done with a polishing fluid Buechler Micropolish II 0.05 μm (γ-Al$_2$O$_3$ – water suspension). In order to highlight the metal microstructure, the polished surface was etched by 10 % solution of FeCl$_3$ in ethanole.

RESULTS AND DISCUSSION

XRD analysis method is distinguished for a possibility to qualitatively and quantitatively identify variation of alloy elements in carbide phase and sequence of formation of carbide phases. Unfortunately, sensitivity of this method is not sufficient in case of insignificant amounts of carbide

compounds in steel. To increase the concentration of carbide phase in a sample, steel samples should be electrochemically etched, selectively separating different phases [24]. Separation of chemical compounds is based on their different resistance to aggressive environment under electrochemical processes. In heterogeneous alloys each phase is described by the characteristic curve, whereas its solution rate depends on electrolyte composition, electrolysis conditions, current density, etc. [25].

Variation of electrode potential, which occurs when electric current flows through an electrode, is called polarization. Anodic polarization of 12Х1МФ steel was analysed in hydrochloric acid and citric acid and oxalic acid solutions of different concentration. The results are given in Fig. 2.
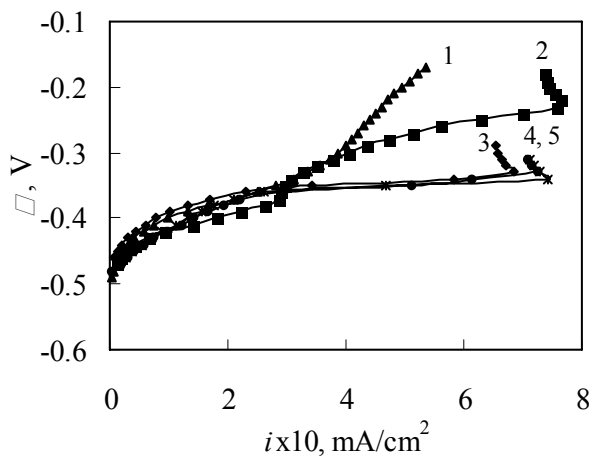

Fig. 2. Anodic polarization curves of steel in electrolyte solutions. Curves: 1 – 0.05 % HCl, 2 – 0.05 % HCl with 0.01 % citric acid, 3 – 0.5 % HCl with 0.05 % citric acid, 4, 5 – 0.5 % HCl with 0.01 % and 0.05 % oxalic acid (φ measured according Ag/AgCl reference electrode)

After analyzing anodic polarization curves in electrolyte solutions, the following electrochemical parameters of 12Х1МФ steel were determined: stationary potential and critical potential and current density, Table 1.

The critical potential defines steel potential limit up to which solution process still prevails, whereas after exceeding it – formation of oxide or salt coating. The most effective etching of steel samples occurs not reaching the above mentioned limit, whereas the biggest critical current density, i. e. 7.55 mA/cm^2 (Fig. 2, curve 2), determined for steel samples in 0.05 % hydrochloric acid with 0.01 % citric acid solution. However, in all electrolyte solutions, excluding hydrochloric acid solution, after reaching the critical current density, anodic solution of steel slows down and the formation of oxide or salt coating begins to prevail.

Taking into account the results of anodic polarization experiments, hydrochloric acid solution was chosen for electrochemical etching of the steel samples.

Microstructure changes of 12Х1МФ steel surface during its ageing were observed using optic microscopy and scanning electron microscopy methods.

In optical microscopy photos (Fig. 3, picture 1) of untreated steel pearlite and ferrite grains are observed, however it is hard to identify fine carbide compositions. High temperature ferrite and pearlite grains begin to

decompose and in their limits the chains (Fig. 3, pictures 2 – 6) of alloyed carbides are formed, which are difficult to see in pictures since both the resolution, depth of field and range of magnifications (to about 550×) of the light microscope are not sufficient.

Table 1. Electrochemical parameters of 12Х1МФ steel in electrolytes solutions

No.	Electrolyte solution	Stationary potential, V	Critical potential, V	Critical current density ×10,mA×cm^{-2}
1	0.05 % HCl	–0.470	–0.17	5.37
2	0.05 % HCl + 0.01 % citric a.	–0.495	–0.22	7.55
3	0.5 % HCl + 0.05 % citric a.	–0.460	–0.33	6.84
4	0.5 % HCl + 0.01 % oxalic a.	–0.484	–0.33	7.42
5	0.5 % HCl + 0.05 % oxalic a.	–0.481	–0.33	7.42

The ongoing structure changes of samples and nucleation of voids may be analysed in an objective way with the scanning electron microscope. In SEM pictures (Fig. 4) the steel ferrite-pearlite structure can be clearly seen. After treating the sample for 384 h at 700 °C, the pearlitic structure partially decomposes (Fig. 4, picture 2), whereas in the photo of the sample treated for 227000 h at 550 °C, a full disintegration of pearlitic structure (Fig. 4, picture 3) is recorded.

XRD analysis was used to confirm carbides formation in steels during their ageing as well as to perform kinetics research. According to the steel critical current density, determined by anodic polarization method, steel etching operating current density was chosen. Its value corresponds to approximately half critical current density. Since for real samples due to approximately 10 times bigger surface area the analysed 0.05 % electrolyte concentration was too small (steel solution process ended very quickly, when a sufficient amount of carbide phase had not yet been released), it was increased up to 5 %.

Fig. 5 shows X-ray diffraction patterns of electrolytically extracted residues of specimens during the early stages of tempering at 600 °C. After 48 h tempering exposure, intensity of diffraction peaks of Fe$_3$C, VC and traces of M$_{23}$C$_6$ (M stands for metals: iron, chromium, molybdenum and vanadium) remains almost unchanged but small amount of M$_7$C$_3$ has been detected (Fig. 5, curve 2). After 216 h accelerated ageing the diffraction peak of carbide M$_{23}$C$_6$ considerably increases (Fig. 5, curve 3) while Fe$_3$C diffraction peak marginally diminishes. The most significant changes have been identified after 654 h isothermal ageing (Fig. 5, curve 5). The intensity of M$_{23}$C$_6$, VC and M$_7$C$_3$ diffraction peaks considerably increase, while Fe$_3$C significantly decreases. All the data showed that tempering causes the Fe-rich M$_3$C carbide (the kinetically favoured phase in the pearlite) to transform to more thermodynamically favoured carbides, rich in Cr and Mo. The most thermodynamically stable carbide M$_6$C was not yet identified.
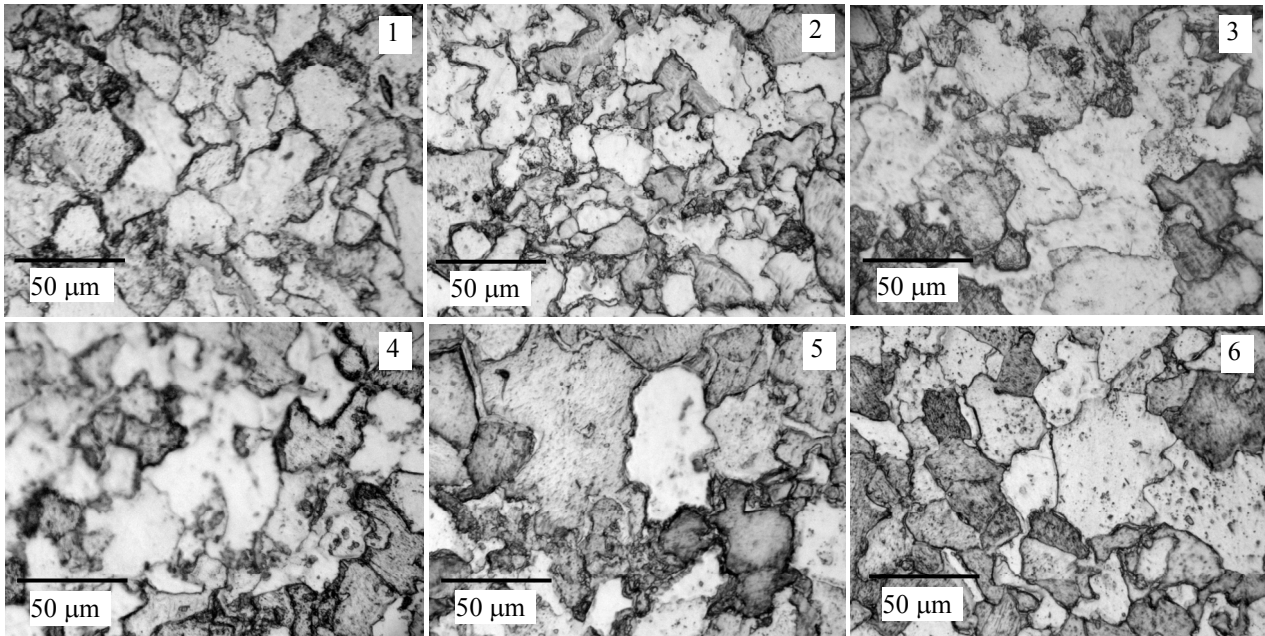
Fig. 3. Optical microstructure of 12X1МФ steel tempered at 700 °C (hours) and etched by 10 % ferrous (III) chloride solution: 1 – virgin steel, 2 – 24, 3 – 48, 4 – 144, 5 – 384 hours, 6 – exploited 227000 hours at 550 °C
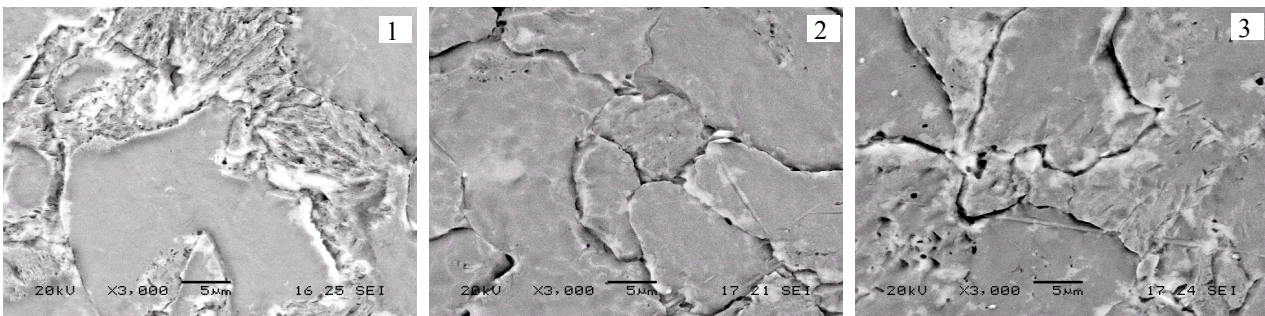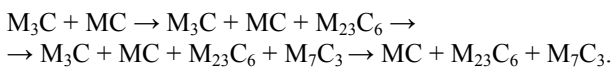

Fig. 4. Microstructure (SEM) of 12X1МФ steel tempered at 700 °C: 1 – virgin state, ferrite-pearlite; 2 – 384 h heated, partial disintegration of pearlitic structure; 3 – 227000 h exploited at 550 °C, full disintegration of pearlitic structure

The sequence observed may be summarized as follows:

$$M_3C + MC \rightarrow M_3C + MC + M_{23}C_6 \rightarrow$$
$$\rightarrow M_3C + MC + M_{23}C_6 + M_7C_3 \rightarrow MC + M_{23}C_6 + M_7C_3.$$

According to the X-ray diffraction data, there are differences in the carbide precipitation evolution among the 2.25Cr1Mo (Cr = 2.16 %), 3Cr1.5Mo (Cr = 2.98 %) steels reported in the previous experimental work [20] and our investigated steel 12X1МФ (Cr = 1.1 %). In the 2.25Cr1Mo steel, M_2C have been detected earlier than M_7C_3 and in 3Cr1.5Mo steel M_2C follows the formation of M_7C_3, while in 12X1МФ steel MC (VC) was found instead of M_2C. However, the sequence of carbide phase evolution obtained here was the same as reported in paper [3] for exploited 12X1МФ steels, which have been collected from various heat and power plants in Ukraine and other parts of the former Soviet Union.

After further performing XRD analysis of the samples, it was determined that during ageing of 12X1МФ steel at 650 °C and 700 °C (Fig. 6 and Fig. 7), the concentration of Fe_3C reduces more rapidly and, at the same time, the rate of transformation to $M_{23}C_6$ alloy carbide is accelerated. No precipitation of stable carbide M_6C was detected too. So, the same carbide precipitation sequence was observed at 650 °C and 700 °C as it was detected at 600 °C, although the precipitation kinetics appears to be faster for all phases at that temperatures. Because the carbide M_6C have been detected in 12X1МФ steel exploited for 227000 h, thus it would be meaningful to continue experiments at elevated temperatures to obtain conditions of full carbide precipitation sequence. These results would be useful for evaluation of steel service time and for prediction remnant life.

In order to evaluate the dependence of above mentioned compounds' amount on ageing time and temperature the integral intensity of diffraction peak of corresponding carbides $M_{23}C_6$ (422) and Fe_3C (031) was evaluated by relative units, whereas dependencies are given in Fig. 8.

The amount of ferrous carbide in steel aged at 600 °C depending on ageing duration changes linearly, whereas at 650 °C and 700 °C it is described by exponential dependencies:
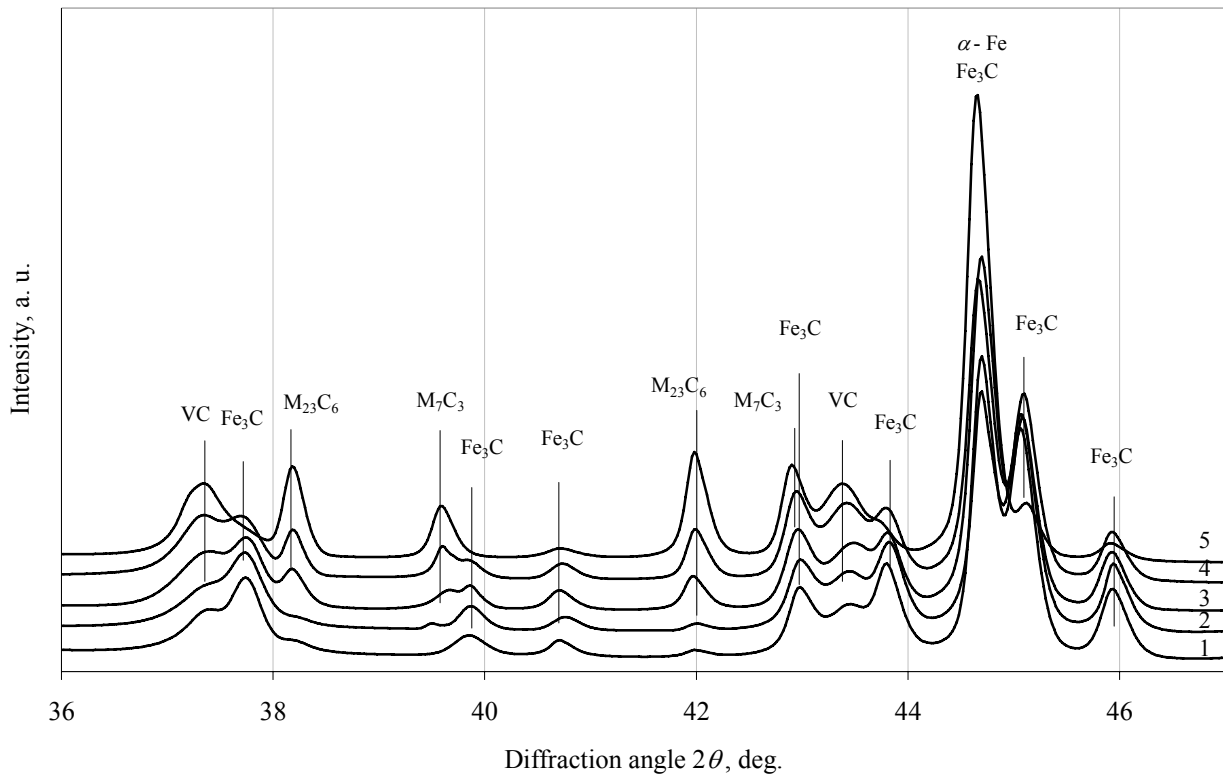
Fig. 5. X-ray diffraction patterns of 12Х1МФ steel tempered at 600 °C. Curves: 1 – virgin steel, 2 – 48 h, 3 – 216 h, 4 – 384 h, 5 – 854 h
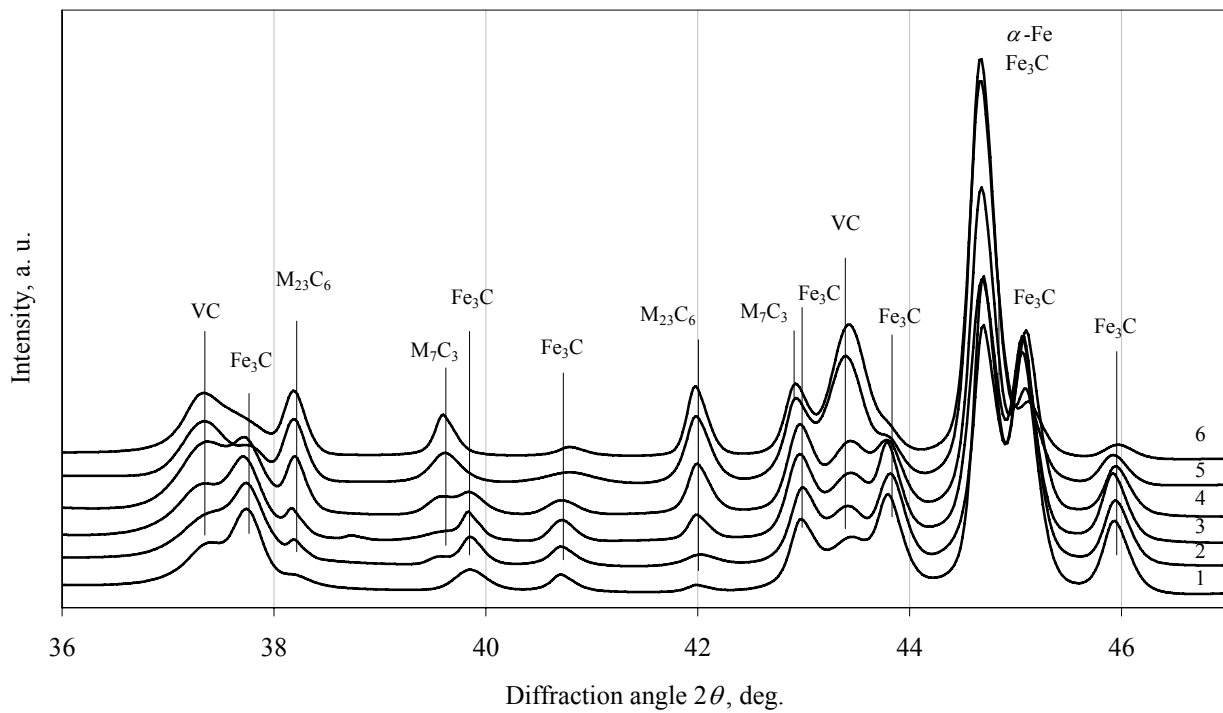

Fig. 6. X-ray diffraction patterns of 12Х1МФ steel tempered at 650 °C. Curves: 1 – virgin steel, 2 – 24 h, 3 – 192 h, 4 – 288 h, 5 – 384 h, 6 – 854 h
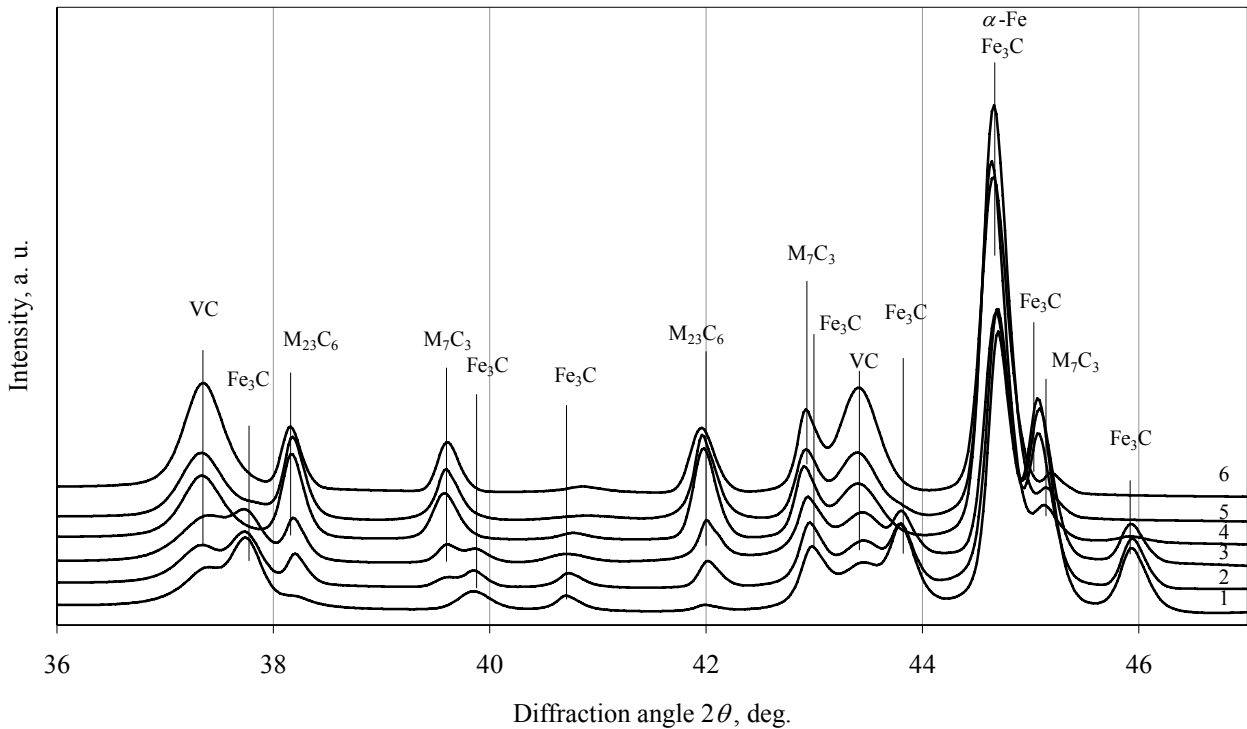
Fig. 7. X-ray diffraction patterns of 12Х1МФ steel tempered at 700 °C. Curves: 1 – virgin steel, 2 – 24 h, 3 – 48 h, 4 – 192 h, 5 – 384 h, 6 – 576 h
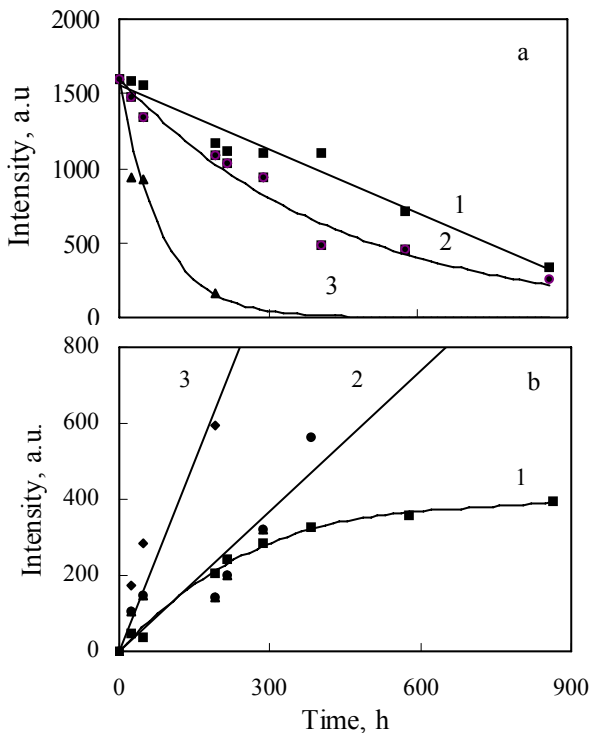

Fig. 8. Dependences of the amount of Fe_3C (a) and $M_{23}C_6$ (b) in 12Х1МФ steel on ageing time and temperature. Curves: 1 – 600 °C, 2 – 650 °C, 3 – 700 °C

Fe_3C

$I_{(031)} = -1.5712\,\tau + 1579$; $T = 600$ °C;

$I_{(031)} = 1602e^{-0.003\,\tau}$; $T = 650$ °C;

$I_{(031)} = 1595\,e^{-0.012\,\tau}$; $T = 700$ °C.

Whereas the amount of $M_{23}C_6$ changes linearly at 650 °C and 700 °C and it is described polynomial at 600 °C temperature:

$I_{(422)} = 9 \cdot 10^{-7}\,\tau^3 - 0.002\,\tau^2 + 1.445\,\tau$, $T = 600$ °C;

$I_{(422)} = 1.2327\,\tau$, $T = 650$ °C;

$I_{(422)} = 3.3308\,\tau$, $T = 700$ °C;

where I is the integral intensity of diffraction peak, a.u., τ is the ageing time, h.

The results of this study make possibility to evaluate state of the equipments in heat and power generating plants, to prevent from sudden failure and predict its service time.

CONCLUSIONS

The microstructure of the steel in the thermal power plants facilities undergoes evolution during long term operation or tempering in laboratory conditions under 600, 650 and 700 °C temperatures. The changes of ongoing structure are difficult to analyze with ordinary methods. To rise the quantitative content of carbide phases the anodic polarization and electrochemical isolation was applied. Anodic polarization of 12Х1МФ steel was analysed in hydrochloric acid solution and parameters of carbide phase electrochemical isolation (critical potential $\varphi_k = -0.17$ V and current density $i_a = 5.37, \times 10$ mA/cm^2) were determined.

During exploitation at 550 °C for 227000 h and ageing at 700 °C for 576 h the steel pearlite completely decomposes – tempering causes the Fe-rich M_3C carbide to transform to more thermodynamically favoured carbides,

rich in Cr and Mo. It was established that the evolutionary sequence of carbides in steel aged in elevated temperatures is the same as in service exploited steel.

XRD analysis of electrochemically separated carbide phase is a rapid and informative method of evaluation the service condition of steel.

RFERENCES

1. **Dzioba, I.** Failure Assessment Analysis of Pipelines for Heat and Power Generating Plants According to the SINTAP Procedures   *International Journal of Pressure Vessels and Piping* 82 2005: pp. 787 – 796.

2. **Robson, J. D.,   Bhadeshia, H. K. D. H.**   Modelling Precipitation Sequences in Power Plant Steels. Part 1: Kinetic Theory   *Materials Science and Technology*   13 1997: pp. 631 – 639.

3. **Singh, R., Singh, S. R.** Remaining Creep Life Study of Cr-MO-V Main Steam Pipe Lines   *Int. J. Pres. Ves. & Piping* 73 1997: pp. 89 – 95.

4. **Robson, J. D.,   Bhadeshia, H. K. D. H.**   Kinetics of Precipitation in Power Plant Steels *Calphad* 20 (4) 1996: pp. 447 – 460.

5. **Zhao, J., Han, S., Gao, H., Wang**, **L.** Remaining Life Assessment of a CrMoV Steel Using the Z-parameter Method   *International Journal of Pressure Vessels and Piping* 81 2004: pp. 757 – 760.

6. **Jayana, V., Khanb, M. Y., Husain**, **M.** Coarsening of Nano Sized Carbide Particles in 2.25Cr–1Mo Power Plant Steel after Extended Service   *Materials Letters* 58 2004: pp. 2569 – 2573.

7. **Jie Zhao, Shuang-qi Han, Hong-bo Gao, Lai Wang.** Remaining Life Assessment of a CrMoV Steel Using the Z-parameter Method   *International Journal of Pressure Vessels and Piping* 81 2004: pp. 757 – 760.

8. **Thomson, R. C., Bhadeshia, H. K. D. H.**   Changes in Chemical Composition of Carbides in 2-25Cr-1 Mo Power Plant Steel. Part 1: Bainitic Microstructure   *Materials Science and Technology* 10 1994: pp. 193 – 203.

9. **Race, J. M.,   Bhadeshia, H. K. D. H.**   Precipitation Sequences during Carburisation of Cr-Mo Steel   *Materials Science and Technology* 8 1992: pp. 875 – 882.

10. **Thomson, R. C., Bhadeshia, H. K. D. H.** Changes in Chemical Composition of Carbides in 2-25Cr-1 Mo Power Plant Steel. Part 2: Mixed Microstructure *Materials Science and Technology* 10 1994: pp. 205 – 208.

11. **Robson, J. D.,   Bhadeshia, H. K. D. H.**   Modelling Precipitation Sequences in Power Plant Steels. Part 2: Application of Kinetic Theory   *Materials Science and Technology* 13 1997: pp. 640 – 644.

12. **Vyrostkova, A., Kroupa, A., Janovec, J., Svoboda, M.** Carbide Reactions and Phase Equilibria in Low Alloy Cr-Mo-V Steels Tempered at 773 – 993 K.   Part I: Experimental Measurements *Acta. Matter* 46 (1) 1998: pp. 31 – 38.

13. **Kroupa, A., Vyrostkova, A., Svoboda, M., Janovec, J.** Carbide Reactions and Phase Equilibrium in Low Alloy Cr-Mo-V Steels Tempered at 773 – 993 K. Part 11: Theoretical Calculations *Acta. Matter* 46 (1) 1998: pp. 39 – 49.

14. **Fujita, N.** Modelling Carbide Precipitation in Alloy Steels. A Dissertation Submitted for the Degree of Doctor of Philosophy at the University of Cambridge 2000: p. 216.

15. **Miyata, K., Sawaragi, Y.** Effect of Mo and W on the Phase Stability of Precipitates in Low Cr Heat Resistant Steels *ISIJ International* 41 (3) 2001: pp. 281 – 289.

16. **Homolova, V, Janovec, A. J., Kroupa, A.** Experimental and Thermodynamic Studies of Phase Transformations in Cr–V Low Alloy Steels *Materials Science and Engineering A* 335 2002: pp. 290 – 297.

17. **Homolova, V., Janovec, J., Zahumensky, P., Vyrostkova, A.** Influence of Thermal-deformation History on Evolution of Secondary Phases in P91 Steel *Materials Science and Engineering A* 335 2002: pp. 1 – 7.

18. **You Fa Yin, Faulkner, R. G.** Modelling the Effects of Alloying Elements on Precipitation in Ferritic Steels *Materials Science and Engineering A* 344 2003: pp. 92 – 102.

19. **Dobrzanski, J.** The Classification Method and the Technical Condition Evaluation of the Critical Elements' Material of Power Boilers in Creep Service Made from the 12Cr–1Mo–V *Journal of Materials Processing Technology* 164 – 65 2005: pp. 785 – 794.

20. **Baker, R. G., Nutting, J.** The Tempering of 2.25Cr–1Mo Steel after Quenching and Normalising *Journal of the Iron and Steel Institute* 192 1959: pp. 257 – 268.

21. **Fujita, N, Bhadeshia, H. K. D. H.** Modelling Simultaneous Alloy Carbide Sequence in Power Plant Steels *ISIJ International* 42 (7) 2002: pp. 760 – 769.

22. PDF – 2 International Centre for Diffraction Data 12 Campus Boulevard Newtown Square, PA 19073 – 3273, USA.

23. **Cheary, R. W., Coelho, A. A.** Programs XFIT and FOURYA. Deposited in CCP14 Powder Diffraction Library, Engineering and Physical Sciences Research Council, Daresbury Laboratory, Warrington, England, 1996 (http://www.ccp14.ac.uk/tutorial/xfit-95/xfit.htm).

24. **Trusov, L. P., Bogatirev, Ju. M., Jeremina, V. P., Uporova, V. A., Ashichmina, L. A., Lepechin, A. Z.** Repair of Thin Structure and Properties of 12X1MФ Steel after Sustained Exploitation *Teploenergetika* 1 (3) 1976: pp. 69 – 71 (in Russian).

25. **Chylinska, R., Garbiak, M., Piekarski, B.** Electrolyte Phase Extraction in Stabilised Austenitic Cast Steel *Materials Science* (*Medžiagotyra*) 4 (11) 2005: pp. 348 – 351.